Angular dependence of x-ray absorption spectrum for field-aligned iron-based superconductors

B. C. Chang, Y. B. You, T. J. Shiu, M. F. Tai, and H. C. Ku*
Department of Physics, National Tsing Hua University, Hsinchu 30013, Taiwan

Y. Y. Hsu
Department of Physics, National Taiwan Normal University, Taipei 10677, Taiwan

L. Y. Jang and J. F. Lee
National Synchrotron Radiation Research Center, Hsinchu 30076, Taiwan

Z. Wei, K. Q. Ruan, and X. G. Li
Hefei National Laboratory for Physical Sciences at Microscale and Department of Physics, University of Science and Technology of China, Hefei 230026, China
(Received 3 July 2009; revised manuscript received 9 September 2009; published 5 October 2009)

Anisotropic Fe *K*-edge and As *K*-edge x-ray absorption near-edge spectrum measurements on superconducting (T_c=52 K) $(Sm_{0.95}La_{0.05})FeAs(O_{0.85}F_{0.15})$ field-aligned microcrystalline powder are presented. The angular dependence of Fe pre-edge peak (dipole transition of Fe 1*s* electrons to Fe 3*d*/As 4*p* hybrid bands) relative to the tetragonal *ab* plane of aligned powder indicates larger density of state along the *c* axis and is consistent with the local-density approximation band-structure calculation. The anisotropic Fe *K*-edge spectra exhibit a chemical shift to lower energy compared to FeO which are closely related to the itinerant character of Fe^{2+} $3d^6$ orbitals. The anisotropic As *K*-edge spectra are more or less the mirror images of Fe *K* edge due to the symmetrical Fe-As hybridization in the FeAs layer. Angular dependence of As main peak (dipole transition of As 1*s* electrons to higher-energy hybrid bands) was observed suggesting character of As 4*d* e_g orbitals.

DOI: 10.1103/PhysRevB.80.165108 PACS number(s): 74.70.−b, 74.25.Jb

I. INTRODUCTION

High-T_c superconductivity with transition temperature T_c up to 55 K was reported in the discovered iron-based RFeAs$(O_{1-x}F_x)$ (rare earth R=La, Ce, Pr, Nd, Sm, or Gd) system.[1–15] The ZrCuAsSi-type (1111) tetragonal structure (space group $P4/nmm$) is a layered structure where the metallic FeAs layers are separated by the insulating $R(O_{1-x}F_x)$ layers. The discovery of the iron-based superconductors has generated enormous interest since these compounds are the noncuprate high-T_c superconductors with T_c higher than 50 K. The parent compound LaFeAsO is semimetal which shows a spin-density wave-type antiferromagnetic order below 150 K after the tetragonal to orthorhombic structural transition.[5] Electron doping to the FeAs layer through partial F^- substitution in the O^{2-} site suppresses both the structural distortion and the magnetic order in favor of superconductivity.[1,3] The phase diagram of the RFeAs$(O_{1-x}F_x)$ system (R=La, Ce, and Sm) provided a useful comparison with the phase diagram of the high-T_c cuprate system.[9–12]

The FeAs layer is believed to be the superconducting layer of the RFeAs$(O_{1-x}F_x)$ system. Studies on the anisotropic properties are crucial to understanding this iron-based system. Since high-quality single crystals are difficult to grow in the (1111) system, we use the field-rotation alignment method to align the superconducting $(Sm_{0.95}La_{0.05})FeAs(O_{0.85}F_{0.15})$ microcrystalline powder.[8] In this paper, the anisotropic Fe *K*-edge and As *K*-edge x-ray absorption near-edge spectroscopy (XANES) measurements were carried out to investigate the electronic structure of unoccupied FeAs conduction bands of the FeAs layer.

II. EXPERIMENT

The superconducting $(Sm_{0.95}La_{0.05})FeAs(O_{0.85}F_{0.15})$ polycrystalline sample was prepared by solid-state reaction in an evacuated and sealed quartz tube. The tetragonal microcrystalline powder can be aligned at room temperature using the field-rotation method such that the tetragonal *ab* plane [a=0.3936(3) nm] is parallel to the aligned magnetic field B_a and *c* axis [c=0.8495(8) nm] is parallel to the rotation axis.[8]

Magnetization and magnetic-susceptibility data were collected with a Quantum Design 1-T μ-metal shielded $MPMS_2$ or a 7-T MPMS superconducting quantum interference device magnetometer from 2 to 300 K.

The anisotropic XANES for the aligned microcrystalline powder was performed at the Taiwan Light Source (TLS) of the National Synchrotron Radiation Research Center (NSRRC) in Hsinchu, Taiwan, with Fe *K*-edge XANES at BL-16A beamline and As *K*-edge XANES at BL-17C beamline. Both BL-16A and BL-17C beamlines use Si(111) double-crystal monochromator with the energy resolution $\Delta E/E=1.5\times10^{-4}$. The tetragonal *ab* plane of the aligned sample is placed parallel to the electric field **E** of the incident linear-polarized x-ray. Fluorescence data was used and ATHENA program was employed for background removal and normalization of XANES spectra.[16]

III. RESULTS AND DISCUSSION

The anisotropic temperature dependence of molar magnetic susceptibility $\chi_{ab}(T)$ and $\chi_c(T)$ for aligned powder

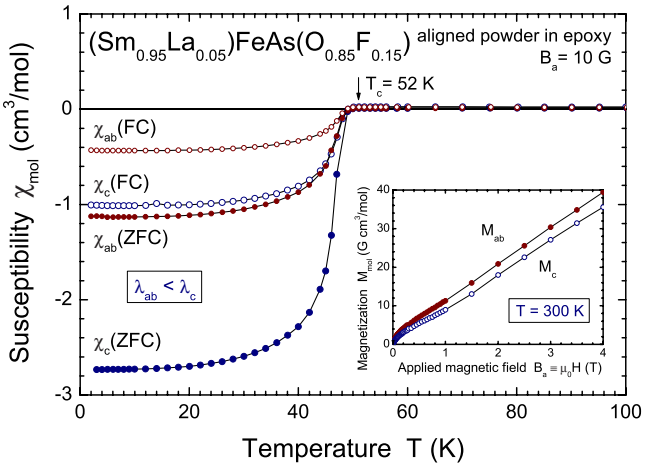

FIG. 1. (Color online) Anisotropic FC and ZFC susceptibility $\chi_{ab}(T)$ and $\chi_c(T)$ at $B_a=10$ G for $(Sm_{0.95}La_{0.05})FeAs(O_{0.85}F_{0.15})$ field-aligned powder. The inset shows the room-temperature anisotropic magnetization $M(B_a)$.

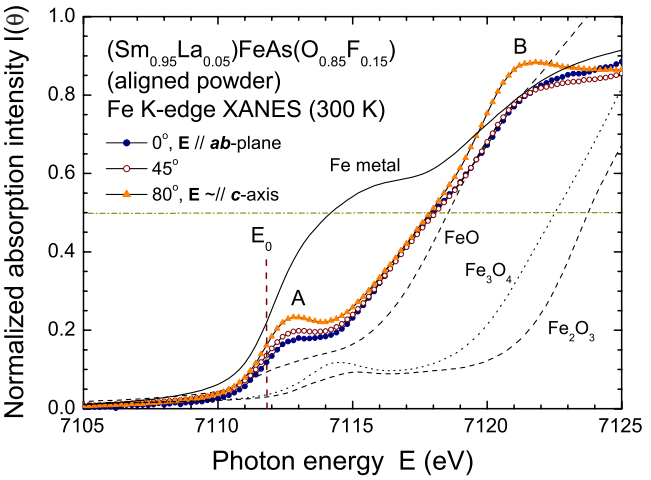

FIG. 2. (Color online) The anisotropic Fe *K*-edge XANES spectra for three orientations of the aligned $(Sm_{0.95}La_{0.05})FeAs(O_{0.85}F_{0.15})$ powder. The zero angle refers to that the electric field **E** of the linear-polarized x-ray is parallel to the tetragonal *ab* plane.

$(Sm_{0.95}La_{0.05})FeAs(O_{0.85}F_{0.15})$ with applied field along the *ab* plane and *c* axis, respectively, are shown collectively in Fig. 1. For dispersed aligned microcrystalline in low applied field of 10 G, both zero-field-cooled (ZFC) and field-cooled (FC) data revealed a sharp superconducting transition temperature T_c of 52 K, which are identical to the T_c measured from bulk polycrystalline sample. Large ZFC intragrain Meissner shielding signals were observed with nearly constant $\chi_c=-2.72$ cm^3/mol and $\chi_{ab}=-1.13$ cm^3/mol up to 20 K. The anisotropic diamagnetic parameter $\gamma=\chi_c/\chi_{ab}$ of 2.4 was deduced for the aligned microcrystalline. The FC flux-trapped signal gave the same anisotropic parameter γ of 2.4. Taking into account the imperfect alignment factor (80%), a larger anisotropic diamagnetic parameter $\gamma\sim 3$ was estimated for a perfectly aligned specimen.[8]

The anisotropic Fe *K*-edge spectra for three orientations of the aligned $(Sm_{0.95}La_{0.05})FeAs(O_{0.85}F_{0.15})$ powder at room temperature are shown in Fig. 2. The zero angle ($\theta=0°$) refers to that the electric field **E** of the linear-polarized x-ray is parallel to the tetragonal *ab* plane. Four standards FeO (Fe^{2+}), Fe_3O_4 ($Fe^{2+/3+}$), Fe_2O_3 (Fe^{3+}), and Fe metal (with standard inflection point of 7112 eV) are also presented for reference.

The general feature of the anisotropic Fe *K*-edge spectra are similar to the previously reported unoriented random powder data for isostructural $LaFeAs(O_{1-x}F_x)$ samples.[13] Two distinct features of absorption peaks, marked A and B, are observed in Fig. 2. The pre-edge peak A, which is near the inflection point $E_0=7111.8$ eV, relates to the transition of Fe 1*s* core electron to the unoccupied Fe 3*d*/As 4*p* hybrid bands. The main peak B, which rides on top of the step-onset feature associated with transitions to continual states, relates to the dipole transition to Fe 4*p*/As 4*d* hybrid bands at higher energy. The energy resolution power ΔE for Fe *K*-edge spectra is around 1 eV due to the monochromator used.

The region between the pre-edge peak A and main peak B is referred to as the main edge. Tracking the chemical shift of the main edge to lower energy is a standard tool for probing variations in formal valence of Fe ions. To compare the chemical shift of the superconducting aligned sample with four standards, a horizontal dashed line at 50% of the relative absorption intensity is drawn in Fig. 2. All three anisotropic $(Sm_{0.95}La_{0.05})FeAs(O_{0.85}F_{0.15})$ spectra are close to the FeO (Fe^{2+}) standard but are shifted slightly to lower energy. It is consistent with itinerant character of Fe^{2+} $3d^6$ orbital in the FeAs conduction layer for the electron doped (with some Fe^{1+} $3d^7$ character) $(Sm_{0.95}La_{0.05})FeAs(O_{0.85}F_{0.15})$ superconductor.

The pre-edge A spectral feature involve transitions of Fe 1*s* core electron into unoccupied final states of Fe 3*d* either through quadrupole or dipole transitions. Since the Fe 1*s* to 3*d* quadrupole transition is weak, the observed strong pre-edge peak A indicates that the local $FeAs_4$ tetrahedral ligand field explicitly allows the dipole transition into unoccupied Fe 3*d*/As 4*p* hybrid bands with bandwidth ~ 3 eV above the inflection point E_0.

Modest angular dependence of Fe *K*-edge spectra was observed. For the anisotropic pre-edge peak A relative to the tetragonal *ab* plane of aligned powder, larger density of state (DOS) of unoccupied Fe 3*d*/As 4*p* conduction bands close to the *c* axis ($\theta=80°$) is observed. This result is consistent with the local-density approximation (LDA) band-structure calculation for this moderately correlated electron system.[7] The peak A maximum of 7112.8 eV for $\theta=80°$ and 7113 eV for $\theta=0°$ were observed. Similar angular dependence was observed in the main peak B with higher DOS for Fe 4*p*/As 4*d* hybrid bands along the *c* axis.

Figure 3 shows the difference spectra (ΔI) which are obtained by subtracting the $\theta=0°$ spectrum from other Fe *K*-edge spectra. Two features labeled ΔA and ΔB in the Fig. 3. The large peak ΔA at $\theta=80°$ indicates a large DOS and large hybridization along the *c* axis. A large peak ΔB for $\theta=80°$ indicates a large 1*s*-4*p* absorption edge.

Low-temperature anisotropic Fe *K*-edge measurements, either below or above $T_c=52$ K (at 10 and 100 K, respec-

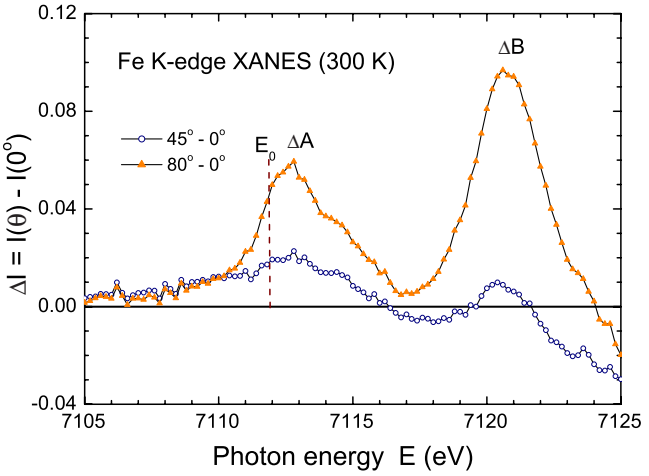

FIG. 3. (Color online) The difference spectra (ΔI) obtained by subtracting the θ=0° data from the other spectra.

tively), gives similar pre-edge A feature as the room-temperature data in Fig. 4. The DOS of unoccupied Fe $3d$/As $4p$ hybridization above the Fermi level is unaffected by temperature, which is an indication that the Fe $3d_{xz}$, $3d_{yz}$ character dominates from normal to superconducting state. LDA band calculation indicates a Fermi surface comprised of doubly degenerate hole pocket centered at Γ point and a doubly degenerate electron pocket centered at M point, with dominant Fe $3d_{xz}$, $3d_{yz}$ characters.[7,14]

The anisotropic As K-edge XANES spectra for five orientations of the aligned $(Sm_{0.95}La_{0.05})FeAs(O_{0.85}F_{0.15})$ powder at room temperature are shown collectively in Fig. 5. Again, the zero angle refers to that the electric field **E** of the linear-polarized x-ray is parallel to the tetragonal ab plane. The As metal standard (with standard inflection point of 11 867 eV) is also presented.

The anisotropic As K-edge spectra are more or less the mirror images of Fe K-edge data due to the Fe $3d$/As $4p$ hybridization in the FeAs conducting layer. The energy resolution power for As K-edge spectra decreases to $\Delta E \sim 2$ eV due to higher energy level. Similar to the Fe K-edge data, two distinct features A and B are clearly visible in Fig. 5. The pre-edge peak A at the onset is related to the As $1s$ dipole transition to the unoccupied As $4p$/Fe $3d$ hybrid bands above the inflection point E_0=11 867 eV. The main peak B is the transition to higher energy unoccupied hybrid bands with observable As $4d$ e_g character.

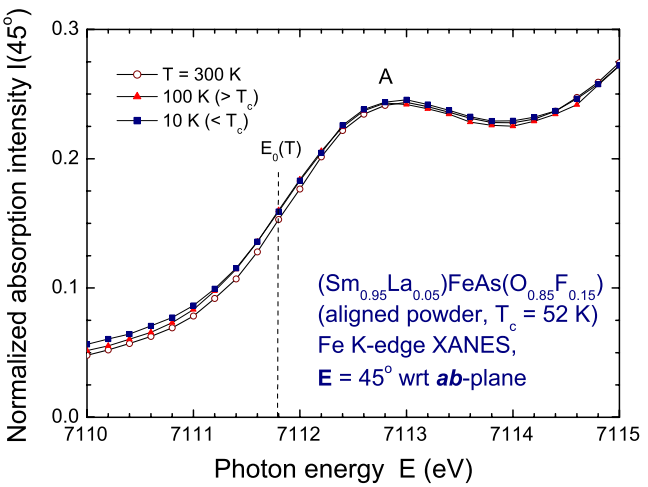

FIG. 4. (Color online) The Fe K-edge XANES spectra (θ=45°) for $(Sm_{0.95}La_{0.05})FeAs(O_{0.85}F_{0.15})$ at 10, 100, 300 K. Low-energy resolution (~1 eV) of these data fails to resolve the small s-wave superconducting gap ($E_g \sim 0.01$ eV) below T_c (Ref. 6).

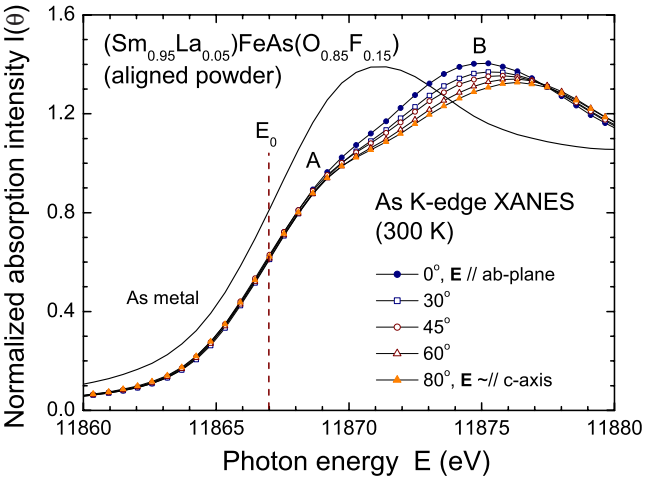

FIG. 5. (Color online) The anisotropic As K-edge spectra for five orientations of the aligned $(Sm_{0.95}La_{0.05})FeAs(O_{0.85}F_{0.15})$ powder.

Weak angular dependence was observed for the pre-edge A feature of As K-edge spectra. However, stronger angular dependence was seen on main peak B indicates a larger DOS along the ab planes with peak maximum at 11 875 eV which suggests a hybrid band with As $d_{x^2-y^2}$ characters. Larger DOS along the c axis with a peak maximum at the slightly higher 11 876.5 eV was observed suggesting a hybrid band with $d_{3z^2-r^2}$ character.

Figure 6 shows the difference spectra (ΔI) which are obtained by subtracting the θ=0° spectrum from other As K-edge spectra. Two features labeled ΔA and ΔB in the Fig. 6. The ΔA for θ=45° has a large DOS and indicates the

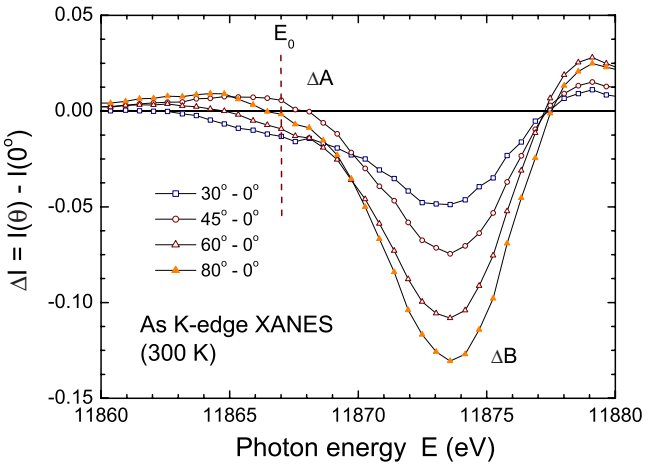

FIG. 6. (Color online) The difference spectra (ΔI) obtained by subtracting the zero angle spectrum from the other spectra

hybridization direction of Fe $3d$/As $4p$ bond. The ΔB decreases with the orientation angles and indicates the large $1s$-$4p$ absorption edge of As K-edge spectra along the ab plane.

IV. CONCLUSION

In conclusion, anisotropic Fe K-edge and As K-edge XANES measurements on superconducting $(Sm_{0.95}La_{0.05})FeAs(O_{0.85}F_{0.15})$ aligned microcrystalline powder are presented. Angular dependence of Fe pre-edge peak A indicates a larger DOS along the tetragonal c axis and is consistent with the LDA band-structure calculation. The anisotropic Fe K-edge spectra exhibits a chemical shift to lower photon energy which is closely related to the itinerant character of Fe $3d$ orbitals. Angular dependence of As main peak B (dipole transition of to higher-energy unoccupied hybrid bands) was observed suggesting character of As $4d$ e_g orbitals.

ACKNOWLEDGMENTS

This work was supported by Grant No. NSC95-2112-M-007-056-MY3, No. NSC97-2112-M-003-001-MY3, No. NSC98-2811-M-007-040 of National Science Council of Republic of China, Grant No. NSFC50421201 of National Natural Science Foundation of China, and Grant No. MSTC2006CB601003, No. MSTC2006CB922005 of Ministry of Science and Technology of China.

*hcku@phys.nthu.edu.tw

[1] Y. Kamihara, T. Watanabe, M. Hirano, and H. Hosono, J. Am. Chem. Soc. **130**, 3296 (2008).
[2] H. Takahashi, K. Igawa, K. Arii, Y. Kamihara, M. Hirano, and H. Hosono, Nature (London) **453**, 376 (2008).
[3] Z. A. Ren, G. C. Che, X. L. Dong, J. Yang, W. Lu, W. Yi, X. L. Shen, Z. C. Li, L. L. Sun, F. Zhou, and Z. X. Zhao, EPL **83**, 17002 (2008).
[4] X. H. Chen, T. Wu, G. Wu, R. H. Liu, H. Chen, and D. F. Fang, Nature (London) **453**, 761 (2008).
[5] C. de la Cruz, Q. Huang, J. W. Lynn, J. Y. Li, W. Ratcliff II, J. L. Zarestky, H. A. Mook, G. F. Chen, J. L. Luo, N. L. Wang, and P. C. Dai, Nature (London) **453**, 899 (2008).
[6] T. Y. Chen, Z. Tesanovic, R. H. Liu, X. H. Chen, and C. L. Chien, Nature (London) **453**, 1224 (2008).
[7] G. Xu, W. Ming, Y. Yao, X. Dai, S. C. Zhang, and Z. Fang, EPL **82**, 67002 (2008).
[8] B. C. Chang, C. H. Hsu, Y. Y. Hsu, Z. Wei, K. Q. Ruan, X. G. Li, and H. C. Ku, EPL **84**, 67014 (2008).
[9] R. H. Liu, G. Wu, T. Wu, D. F. Fang, H. Chen, S. Y. Li, K. Liu, Y. L. Xie, X. F. Wang, R. L. Yang, L. Ding, C. He, D. L. Feng, and X. H. Chen, Phys. Rev. Lett. **101**, 087001 (2008).
[10] J. Zhao, Q. Huang, C. de la Cruz, S. Li, J. W. Lynn, Y. Chen, M. A. Green, G. F. Chen, G. Li, Z. Li, J. L. Luo, N. L. Wang, and P. Dai, Nature Mater. **7**, 953 (2008).
[11] H. Luetkens, H.-H. Klauss, M. Kraken, F. J. Litterst, T. Dellmann, R. Klingeler, C. Hess, R. Khasanov, A. Amato, C. Baines, M. Kosmala, O. J. Schumann, M. Braden, J. Hamann-Borrero, N. Leps, A. Kondrat, G. Behr, J. Werner, and B. Büchner, Nature Mater. **8**, 305 (2009).
[12] A. J. Drew, Ch. Niedermayer, P. J. Baker, F. L. Pratt, S. J. Blundell, T. Lancaster, R. H. Liu, G. Wu, X. H. Chen, I. Watanabe, V. K. Malik, A. Dubroka, M. Rossle, K. W. Kim, C. Baines, and C. Bernhard, Nature Mater. **8**, 310 (2009).
[13] A. Ignatov, C. L. Zhang, M. Vannucci, M. Croft, T. A. Tyson, D. Kwok, Z. Qin, and S.-W. Cheong, arXiv:0808.2134 (unpublished).
[14] L. Boeri, O. V. Dolgov, and A. A. Golubov, Phys. Rev. Lett. **101**, 026403 (2008).
[15] K. Kadowaki, A. Goya, T. Mochiji, and S. V. Chong, J. Phys.: Conf. Ser. **150**, 052088 (2009).
[16] B. Ravel and M. Newville, J. Synchrotron Radiat. **12**, 537 (2005).